Dendrochronologia 36 (2015) 49–59

Contents lists available at ScienceDirect

Dendrochronologia

journal homepage: www.elsevier.com/locate/dendro

Original article

Temporal changes in climatic limitation of tree-growth at upper treeline forests: Contrasted responses along the west-to-east humidity gradient in Northern Patagonia

A. Lavergne[a,b,*], V. Daux[a], R. Villalba[b], J. Barichivich[a,c]

[a] Laboratoire des Sciences du Climat et de l'Environnement, CEA-CNRS-UVSQ, 91191, Gif-sur-Yvette, France
[b] Instituto Argentino de Nivología, Glaciología y Ciencias Ambientales, IANIGLA-CONICET, Mendoza, Argentina
[c] School of Geography, University of Leeds, Leeds LS2 9JT, United Kingdom

ARTICLE INFO

Article history:
Received 4 May 2015
Received in revised form 1 September 2015
Accepted 2 September 2015
Available online 1 October 2015

Keywords:
Patagonia
Dendrochronology
VS-Lite model
Precipitation gradient
Nothofagus pumilio

ABSTRACT

Over the last decades, gradual changes in summer climate in the Southern Hemisphere have affected forest growth in contrasting ways in moist and dry regions. Here, we use correlation analysis and a forward process-based model (Vaganov–Shashkin-Lite) to investigate changes in climate limitation of the interannual tree-ring growth of *Nothofagus pumilio* at the upper treeline along a precipitation gradient in northern Patagonia. Patterns of climate limitation vary consistently along the gradient. At mesic and humid treelines, tree-ring growth is positively related to growing season temperature and negatively to precipitation. At xeric treelines, the opposite is observed. Moreover, the climate-growth relations are not stationary. In particular, according to the model, the step decrease in precipitation in 1952 induced an increase of the moisture limitation at the dry edge of the gradient. Correlation analyses evidence that the dependence of growth on moisture after 1952 has enhanced since 1976. While the model consistently reproduces tree-ring width variations over the 1931–1975 period, it does not capture the growth patterns in the following years. Some environmental parameters (cloudiness, snowpack, atmospheric CO_2) affecting moisture, radiation and stomatal aperture may have reached thresholds beyond which the effect on tree-growth has become sizable.

1. Introduction

Changes in summer climate regimes associated with the anomalous positive trend in the Southern Annular Mode (SAM; Archer and Caldeira, 2008) have influenced the patterns of forest growth across much of the extra-tropical Southern Hemisphere (Villalba et al., 2012). Growing seasons in the temperate belt of the Southern Hemisphere have become warmer and drier as the mid-latitude westerly flow has weakened during recent decades (Gillett et al., 2006; Garreaud et al., 2009). Warming has stimulated tree growth in cool and moist subalpine forests of Tasmania and New Zealand (Allen et al., 2014, 2001; Cook et al., 2000; Villalba et al., 2012) whilst drying has reduced growth rates in mesic and dry forests of southern South America (Christie et al., 2011; Mundo et al., 2012; Villalba et al., 2012). Temporal stability of significant correlations between tree-ring chronologies and climatic variables suggest that forests growing at marginal locations, where growth is dominantly limited by either temperature or moisture, have responded consistently to this observed shift in growing season climate (Villalba et al., 2012; Muñoz et al., 2014). However, growth responses of mesic north Patagonian forests and at some treeline locations where temperature and moisture simultaneously co-limit tree-ring growth, appear to be more complex and time-dependent (Daniels and Veblen, 2004; Álvarez et al., 2015; Suarez et al., 2015 Suarez et al., 2015). Warmer conditions and large-scale changes in atmospheric circulation during the late twentieth century have reduced temperature limitation but might have increased moisture limitation, especially for species growing at mesic and humid environments along the north Patagonian precipitation gradient (Suarez et al., 2015).

The beech *Nothofagus pumilio* is the dominant subalpine tree species in northern Patagonia. The radial growth of the species at the upper treeline is typically controlled by spring–summer climate and has been used to reconstruct past temperatures and snow cover duration (Villalba et al., 1997; Lara et al., 2001;

* Corresponding author at: Laboratoire des Sciences du Climat et de l'Environnement, CEA-Orme des Merisiers, Bât 701, Gif-sur-Yvette, 91191, France.
E-mail address: alienor.lavergne@lsce.ipsl.fr (A. Lavergne).

http://dx.doi.org/10.1016/j.dendro.2015.09.001
1125-7865/

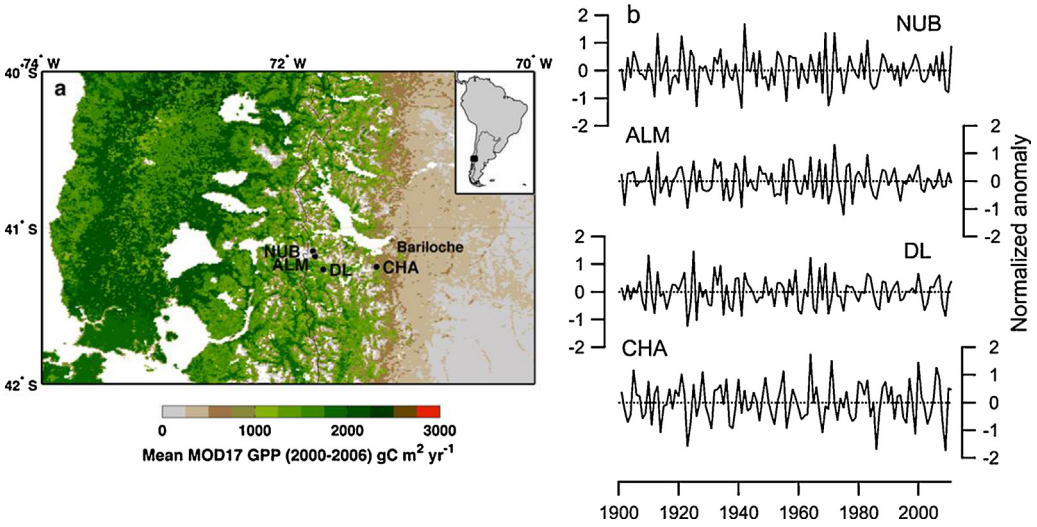

Fig. 1. (a) Location of the tree-ring sites and Bariloche meteorological station along the west-to-east climate and productivity gradient in northern Patagonia. Gross Primary Production (GPP) is based on the MOD17 product (Zhao et al., 2005). (b) Mean standardized tree-ring width chronologies of *Nothofagus pumilio* from northern Patagonia for each site along the west-to-east precipitation gradient (NUB, ALM, DL and CHA) between 1900 and 2011.

Aravena et al., 2002). Yet, correlations between climate and tree-ring growth at some treeline locations in northern Patagonia have been shown to vary substantially between early-20th century cool-wet and current warm-dry climate regimes (Raffaele et al., 1998; Daniels and Veblen, 2004). Furthermore, contrary to the expectation of enhanced growth rates with recent warming, tree growth at an adjacent high-elevation site in the western side of the Andes appears to have declined during recent decades (Álvarez et al., 2015). These observations could suggest a non-linear growth response to temperature or the emerging influence of other environmental controls at some high-elevation forests in the region. Similar site-level temporal instabilities in historical patterns of climate limitation of tree growth have been observed at treeline forests in North America (Ohse et al., 2012; Chavardès et al., 2013), where the so-called tree-ring divergence phenomenon has been described (Jacoby and D'Arrigo, 1995; D'Arrigo et al., 2004, 2008).

The recent development of generic forward models of tree-ring formation offer a new approach for studying the nature of growth responses to climate, overcoming some limitations of traditional linear correlation analyses (Anchukaitis et al., 2006; Boucher et al., 2014; Evans et al., 2013, 2006; Vaganov et al., 2011). These models can represent mixed and non-linear tree growth responses to changing climatic factors from daily to seasonal and decadal time scales. The Vaganov–Shashkin-Lite model (VS-Lite; Tolwinski-Ward et al., 2011) is perhaps the best model available for studying the nature of tree growth in regions were detailed daily climate data and field observations are not readily available. This model requires only monthly precipitation and temperature data to provide a representation of the climatic controls of tree-ring growth based on the principle of limiting factors and non-linear growth response functions (Fritts, 1976). VS-Lite has been used to simulate and evaluate regional patterns of climate limitation of tree growth in a range of environments from semi-arid to temperate and boreal regions (Breitenmoser et al., 2014; Evans et al., 2014; Tolwinski-Ward et al., 2011).

In this study, we combine linear correlation analysis with the VS-Lite model to investigate changes in the climate drivers of *N. pumilio* growth in upper treeline forests along the west-to-east precipitation gradient of northern Patagonia. We address the following question: is water limitation becoming more important than temperature limitation in recent decades with the drier and warmer SAM-driven climate regime, especially in the more moisture-limited environments? In cold and wet environments, we expect the typical pattern of temperature limitation described in previous studies (Villalba et al., 1997) whilst in cold and dry environments toward the east, tree growth should become more limited by water availability. With the persistent positive phase of the SAM, and the concomitant warming and drying in northern Patagonia, we also expect that water limitation should have become more important in recent decades (Daniels and Veblen, 2004; Suarez et al., 2015). This is the first detailed modeling study investigating the controls of tree-ring growth conducted in the region and thus provides novel mechanistic insights into the responses of these austral forests to recent climate change.

2. Material and methods

2.1. Regional setting and study species

Patagonia extends from about 37°S to 55°S and represents the southernmost portion of the South American continent. The regional climate is mainly driven by the interactions between the circum-Antarctic cyclonic belt to the south and the subtropical Pacific high-pressure cell to the northwest. The strong westerlies resulting from the large pressure differences between these semi-permanent circulation features in the atmosphere permanently interact with the north-south mountain range of the Andes (Aceituno, 1988; Villalba et al., 2003; Garreaud et al., 2009). The Andes Cordillera acts as a topographic barrier to the persistent westerlies bringing moisture from the South Pacific Ocean. The air masses discharge most of the humidity in the way up to the mountains on the western slopes of the Andes to descend drier on the eastern slopes. Therefore, the mountain range induces a dramatic decline in mean annual precipitation from 4000 mm at Lago Frías, near the continental divide, to about 500 mm toward the Patagonian steppe (Jobbagy et al., 1995; Veblen, 1979). Gross Primary productivity (GPP) follows the eastward decline in precipitation and ranges from around 2000 g C m^2 $year^{-1}$ in the most productive forests to about 500 g C m^2 $year^{-1}$ in the Patagonian steppe (Fig. 1; Muñoz et al., 2014; Zhao et al., 2005). In northern Patagonia, the annual migratory cycle of the Pacific anticyclone induces strong precipitation seasonality. Precipitation is largely concentrated from

late fall to early spring followed by a drier and mild period during summer and early fall (López Bernal et al., 2012).

N. pumilio, locally known as Lenga, is a light-demanding deciduous tree widely distributed along the Andes from 35°36′S to 56°S in Argentina and Chile (Donoso, 1981). This species usually dominates the upper portion of the altitudinal limit of the woody vegetation. In northern Patagonia, *N. pumilio* grows at elevations ranging from 1100 to 1600 m under a great variety of soils, environmental conditions, and disturbance regimes (Schlatter, 1994). The growing season of the species in the region extends between September and May but its duration decreases with elevation due to the lower temperatures (Rusch, 1993). *N. pumilio* forests develop mainly on fertile soils derived from recent volcanic ashes (Rusch, 1993). In drier sites, roots can reach water-saturated soils or ground water up to 2–3 m depth (Schulze et al., 1996).

2.2. Sampling and tree-ring processing

During the austral summer of 2013, four treeline sites, previously sampled during the 1990s (Villalba et al., 1997, 2003), were re-visited to update the network of tree-ring chronologies in northern Patagonia. Our sampling sites are located along the regional precipitation gradient from Cerro Tronador (41°09′S, 71°53′W) to the drier Challhuaco valley near Bariloche (41°09′S, 71°18′W). From west to east, the sampling sites are Paso de las Nubes (NUB), La Almohadilla (ALM), Diego de León (DL) and Challhuaco (CHA) (Fig. 1; Table 1). The drier, easternmost part of the gradient represents the eastern edge of *N. pumilio* distribution on the leeward flank of the Andes. At each site, at least 30 trees were double-cored at about 1.3 m above ground using a Pressler borer with a diameter of 5 mm.

Since the growing season in the Southern Hemisphere overlaps two calendar years, the date of each ring was assigned to the year when ring growth began (Schulman, 1956). Thus, the last complete tree ring in the cores sampled in the summer of 2013 was dated to the year 2011 because the 2012 tree ring was still incomplete. Overall, more than 500 cores were examined and cross-dated following standard dendrochronological procedures (Stokes and Smiley, 1968). Quality-control and accuracy of measurements and cross-dating were conducted with the COFECHA program (Holmes, 1983). Cross-dated tree-ring width series were detrended and indexed using a 10-year fixed-length cubic smoothing spline implemented in the CRUST routine (Melvin and Briffa, 2014a,b, 2008) in order to retain only inter-annual variability in the chronologies and filter out multi-decadal trends. The standardized series at each site were averaged to produce a mean site chronology. The descriptive statistics of the individual tree-ring chronologies are shown in Table 1.

The Expressed Population Signal statistic (EPS; Briffa, 1984; Wigley et al., 1984) was calculated to assess in the chronology the strength of the common growth signal over time. Based on EPS (>0.85) and sample depth (10 has been arbitrarily considered as a minimum number of trees), the optimal common period between chronologies was 1785–2011 (Table 1). The first Empirical Orthogonal Function (EOF), referred as to the leading pattern of growth variability, was computed from the correlation matrix of the four tree-ring chronologies to evaluate the spatiotemporal patterns of tree growth across the transect over the period 1785–2011.

2.3. Climatic limitation of tree growth

Temperature and moisture controls of tree-growth variability were first empirically identified using simple and partial correlations (Meko et al., 2011) between individual tree-ring chronologies and monthly temperature and precipitation from the nearest meteorological station at Bariloche (41°09′S–71°10′W, 840 m asl; Servicio Meteorológico Nacional, Fig. 1) over the 1934–2009 period. The station records were homogenized and gap-filled using the R routine HOMER (HOMogenization softwarE in R; Mestre et al., 2013; Venema et al., 2013) and climatic series from additional stations located in the area (40–43°S and 71–73°W). The use of partial correlation allows assessing the relationship between two variables while controlling for the effects of a third variable. In our region, the mean temperature is negatively correlated with total precipitation in summer (DJFM; $r = -0.57$, $p < 0.01$) therefore partial correlations between tree-ring growth and precipitation controlling by temperature were computed. Correlations were computed for 18 months from October of the year prior to ring formation to March of the current year. The significance of each correlation was evaluated using bootstrapping with 1000 Monte Carlo simulations (Ebisuzaki (1997)).

We also used the VS-Lite forward model version 2.3 (Tolwinski-Ward et al., 2011; available at http://www.ncdc.noaa.gov/paleo/softlib/softlib.html) to mechanistically identify the climate controls of tree-growth and simulate tree-ring chronologies as a function of climate. VS-Lite is a simplified version of the full Vaganov–Shashkin forward model (Vaganov et al., 2011; 2006) implemented in Matlab. It simulates annual tree-ring width using the principle of limiting factors and requires for input only latitude, monthly mean temperature, and monthly total precipitation. The model estimates monthly soil moisture from temperature and total precipitation data via the empirical one-layer Leaky Bucket model of hydrology (Huang et al., 1996). Snow dynamics are not considered in the model and thus all precipitation is assumed to be liquid. Seasonal insolation or day length is determined from site latitude and does not vary from year-to-year. For each year, the model simulates standardized (ageless) tree-ring width anomalies from the minimum of the monthly growth responses to temperature (gT) and moisture (gM), modulated by insolation (gE).

In this study, most of the tuneable model parameters (e.g., soil moisture, runoff, root depth) were set to the default values proposed in Tolwinski-Ward et al. (2011). The growth response functions for temperature (gT) and moisture (gM) in VS-Lite involve only two parameters. The first parameter represents the temperature (T_1) or moisture (M_1) threshold below which growth will not occur, while the second is the optimal temperature (T_2) or moisture (M_2) above which growth is not limited by climate. Unlike the full version of the VS model, VS-Lite does not have an upper threshold in the growth response functions above which the influence of temperature and moisture turns negative. The growth function parameters were estimated for each site via Bayesian calibration over the entire period with climatic data between 1931 and 2008. For this, the model was evaluated 15,000 times for each site using three parallel Markov Chain Monte Carlo (MCMC) chains with uniform prior distribution for each parameter and a white Gaussian noise model error (Tolwinski-Ward et al., 2013). The posterior median for each parameter was used to obtain the "calibrated" growth response for a given site. Finally, the model was run over the entire period 1931–2008 using the calibrated parameters for each site to produce a simulated tree-ring chronology that represents an estimate of the climate signal of tree growth. To compute annual ring widths, we integrated the overall simulated growth rates (i.e., the point-wise minimum of monthly gT, gM and gE) over the period between previous-year March and current-year June.

To evaluate the temporal stability of the calibrated growth response functions, we divided the period 1931–2008 into two equal 39-year intervals and withhold the second half for validation of the parameters estimated in the fist half. In addition, we conducted series of calibrations over a 21-year sliding window from 1931 to 2008 to detect the timing of changes in growth parameters observed at some sites with complex climate responses.

Table 1
Location and descriptive statistics of the four tree-ring chronologies of *N. pumilio* used in this study. Sampling sites are Paso de las nubes (NUB), La Almohadilla (ALM), Diego de León (DL) and Challhuaco (CHA).

Site	Lat. S	Lon. W	Elevation m asl	Cores	Period	EPS[a] >0.85	Mean *r*	AR1[b]	EOF1[c] Loading
NUB	41°09′	71°48′	1274	86	1644–2011	1750	0.49	0.52	0.64
ALM	41°11′	71°47′	1425	170	1539–2011	1595	0.52	0.62	0.85
DL	41°16′	71°39′	1520	156	1546–2011	1634	0.60	0.55	0.83
CHA	41°15′	71°17′	1612	135	1670–2011	1785	0.53	0.55	0.71

[a] Expressed population signal.
[b] First order autocorrelation.
[c] First Empirical Orthogonal Function.

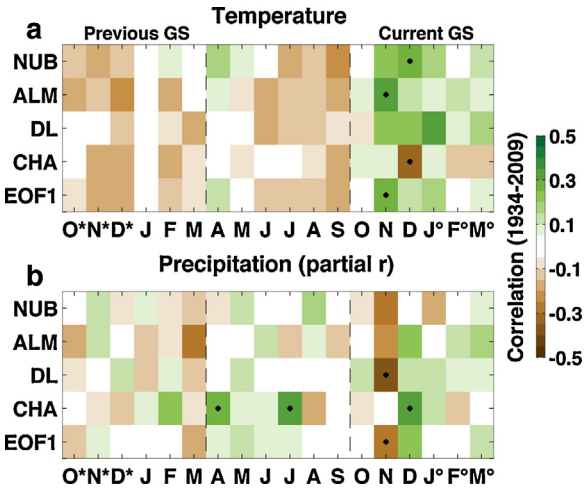

Fig. 2. Tree-ring growth responses to climate over 1934–2009. (a) Simple correlations with temperature and (b) partial correlations with precipitation controlled by temperature. The correlations are calculated from October of the antepenultimate year (*) to March of the following year (°). Correlations are based on 10-year high-pass filtered series. The black points indicate months with significant correlations ($p < 0.05$).

3. Results

3.1. Tree-ring chronologies and their correlation with climate

Tree-growth patterns of *N. pumilio* show common inter-annual variations at the three most mesic sites during the last century (Fig. 1b). The mean series intercorrelation of 0.46 indicates some degree of common interannual variability in tree growth across the gradient. The leading EOF of the four chronologies accounts for 58% of the total variance over the common period showing positive loadings for all chronologies. The two chronologies in the middle part of the gradient (ALM and DL) have the largest loadings (Table 1), indicating that the chronologies at the extremes of the gradient share less common variability. These results suggest that there are some differences in growth variability along the gradient, which imply differences in climate limitation.

Long-term correlations between the tree-ring chronologies and climate indicate that tree-ring growth at the mesic treeline sites (NUB, ALM and DL) is positively associated with temperature during late spring (November/December; $r = 0.31$, $p < 0.05$, at NUB over 1934–2009; Fig. 2) and negatively with precipitation during the same period (November; partial $r = -0.3$, $p < 0.05$, at DL). This indicates that growth is stimulated by warm and dry late spring conditions. In contrast, tree growth at the driest treeline (CHA) is negatively correlated with temperature ($r = -0.31$, $p < 0.05$) and positively with precipitation (partial $r = 0.32$, $p < 0.05$) in December. A significant and positive influence of precipitation on tree growth controlled by temperature is also observed at this site in April and July (partial $r = 0.27$ and 0.32, $p < 0.05$, respectively). Thus, growth at this xeric treeline site is stimulated by cool and wet conditions during early summer and early fall. This result again indicates that limiting factors of tree growth at the wet and dry extremes of the precipitation gradient are substantially different. The leading EOF of the four chronologies is significantly and positively correlated with temperature ($r = 0.27$, $p < 0.05$) and negatively with precipitation (partial $r = -0.27$, $p < 0.05$) in November, and thus it only captures the growth signal of the mesic sites at the middle and western sectors of the precipitation gradient.

The regional climate does not show dramatic trends during the most recent part of the study period. Change-point analysis (Beaulieu et al., 2012) indicates that long-term precipitation and the corresponding soil moisture derived from the VS-Lite model, exhibit a shift towards lower mean values from ca. 1952 onwards, which coincides with the start of the positive trend in the Southern Annular Mode (SAM; Fig. A.1). Temperature anomalies in the region show a significant negative trend of 1.3 °C ($p < 0.01$) between 1945 and 1975 followed by the well-documented step increase around 1976, coincident with the increase in sea surface temperature in the Tropical Pacific Ocean, but with no overall significant warming trend afterwards (0.03 °C for 1976–2008, $p > 0.1$). These changes in mean temperature and precipitation resulted in a warm and wet period before ca. 1952, a period of significant cooling between 1952 and 1975 and a warm and dry period since around 1976.

Sliding correlations between the tree-ring chronologies and modelled moisture reveal that tree growth responses varied substantially among the three different climate regimes identified above (Fig. 3). Tree growth at the two wettest treeline sites (NUB and ALM) shows a consistent shift to negative correlations ($p < 0.1$) with moisture around 1980 over an extended seasonal period that includes most of the previous growth year. Prior to 1980, correlations with moisture are weak or slightly positive, except in the wettest site where correlations with moisture prior to the 1960s are also negative and significant ($p < 0.1$) over most of the previous growth year. Correlations with temperature during the critical November and December months are also temporally instable at these sites (Fig. A.2), and are more significant and positive during the cooling period 1952–1975 (Fig. A.1). In turn, correlations with precipitation become significantly negative in November but significantly positive in December during the warm and dry period 1976–2008 (Fig. A.2).

Tree growth at the site representing the middle of the precipitation gradient (DL) is also predominantly negatively correlated with moisture, but the pattern of temporal instability in the correlations is less clear than in the wettest sites (Fig. 3). Temporal changes in correlation with November and December temperature and precipitation at this site are similar to those at the wettest sites (Fig. A.2). Growth at the driest site (CHA) shows a dramatic change from no moisture sensitivity to strong sensitivity around the early 1970s, with the emergence of significant ($p < 0.1$) and positive correlations during most of the current and previous growth years (Fig. 3). At this site, the relationship between tree-growth and moisture and precipitation in December has been consistently positive since around 1950 (Figs. 3 and A.2). In turn, the correlation with temperature during this month has been consistently nega-

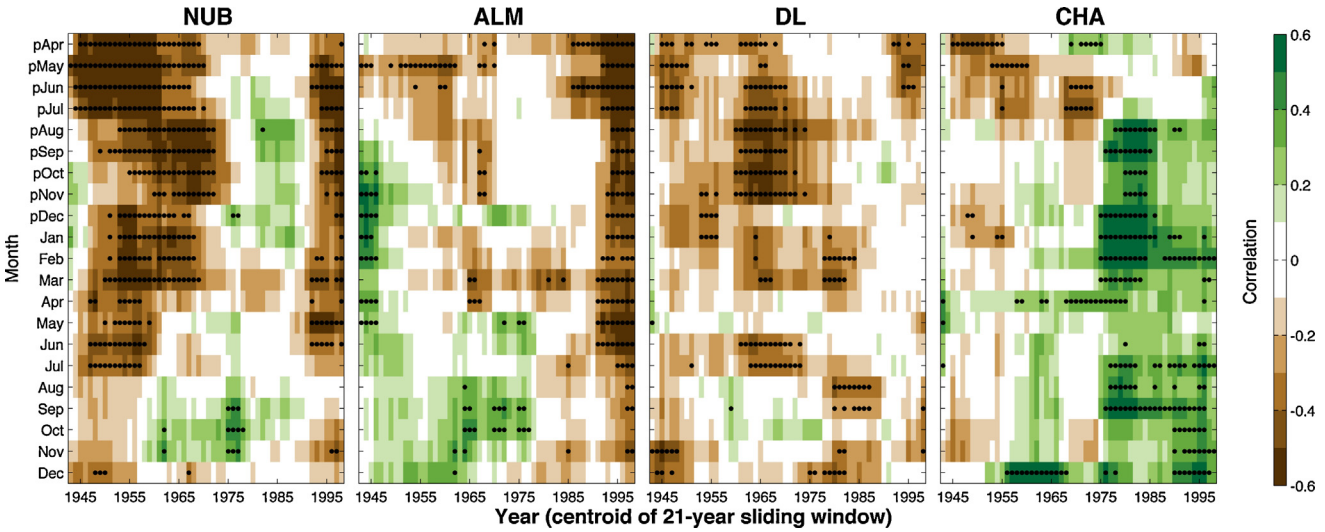

Fig. 3. Temporal patterns of correlation between *N. pumilio* tree-ring growth and soil moisture derived from the VS-Lite model from April of the previous growing year (p) to December of the current growing year. Correlations are shown for 21-year running windows. The stippling denotes significant correlations at the 90% confidence level ($p < 0.1$).

Table 2
Statistics of the Bayesian estimation of the site-by-site tuned VS-Lite growth response parameters T_1, T_2, M_1 and M_2 for the calibration period 1931–1969 and 1931–2008.

	Calib. 1931–1969				Calib. 1931–2008			
	Mean	Min	Max	SD	Mean	Min	Max	SD
T_1 (°C)	5.0	4.4	5.5	0.4	6.1	5.0	6.6	0.8
T_2 (°C)	15.4	14.2	17.1	1.1	14.5	11.7	16.4	2.1
M_1 (v/v)	0.05	0.049	0.054	0.002	0.05	0.05	0.06	0.005
M_2 (v/v)	0.35	0.30	0.36	0.03	0.34	0.30	0.39	0.03

tive and significant until around 1990 when the significance is lost (Fig. A.2).

Overall, the empirical correlation analyses reveal that the climatic response of tree growth at our high-elevation sites varies along the precipitation gradient. The mean patterns of climate response at the sites have also changed significantly through time during the study period, with an emerging positive response to summer precipitation at the wetter sites and a strong increase in moisture limitation at the driest site. Next we attempt to mechanistically model tree growth variability at these sites as a function of climate.

3.2. Forward modeling of tree-ring growth

3.2.1. Model calibration and verification

The Bayesian calibration approach used here provides optimal estimates for the parameters of the growth response function (T_1, T_2, M_1 and M_2) given the model structure, climate data and actual tree ring data for each site. When the model is calibrated over the first half of the study period (1931–1969) all the correlations between the resulting simulated and actual tree-ring chronologies are statistically insignificant during the validation period (1970–2008; Table 3). So the model is not able to simulate the observed tree-ring growth variability at any of the sites in spite of a good skill in all the sites during the calibration period, with a percentage of explained variance of actual growth variability between 14 and 17%.

The lack of validation of the model suggests that the parametrization might be unstable over time. To further investigate this issue and better define the calibration period, the calibration at each site was performed over a sliding window of 21 years between 1931 and 2008. The skill of the parameter set obtained for each window was judged by the correlation between the actual and simulated tree-ring chronologies over the period 1931–2008. The results of this parameterization sensitivity exercise show that the minimum temperature (T_1) and moisture (M_1) parameters for growth are stable over time (not shown). In contrast, the parameters for optimal growth (T_2, M_2) vary substantially during the last two to three decades (Fig. 4).

At the wettest sites, the somewhat unrealistic decrease in calibrated parameters over the last decades (Fig. 4) is related to the observed shift to negative correlations of tree growth with moisture (Fig. 3). Since the simple growth response function of the model does not have an upper threshold beyond which the effect of excessive moisture becomes negative, the Bayesian optimization reduces the moisture threshold for optimal growth to diminish the overall effect of moisture on the simulated growth rates. This results, in turn, on simulated growth being completely limited by temperature, and to further achieve this, the optimization also reduces the temperature threshold for optimal growth. The change in the calibrated optimal moisture parameter at the driest site (Fig. 4b) appears to be related to the shift to increased moisture sensitivity of tree growth at this site in 1975–1976 (Fig. 3). Most of this change in moisture sensitivity in actual tree-ring growth occurred prior to the start of the seasonal window for integration of the simulated growth rates (previous-year March to current-year June). As a result, moisture dynamics during the growing season of the model cannot fully capture the variability of actual tree-ring growth and the optimization tends to adjust for it by reducing the moisture parameter for optimal growth. Indeed, the lagged correlation between the simulated and actual tree-ring chronologies at this site is significant during the second half of the study period regardless of the calibration period used (Table 3).

For all further analyses, we chose to calibrate the model over the entire period of study to obtain a parameter set more representative of the periods of changing growth responses observed in the actual tree-ring chronologies. The values of the calibrated parameters over this long period are consistent with local estimates on the sliding 21-year window, except during the recent periods described above (Fig. 4). The estimated minimum and optimal thresholds for growth averaged across the sites are respectively 6.1 ± 0.8 °C and 14.5 ± 2.1 °C for temperature and 0.05 ± 0.005 v/v and 0.34 ± 0.03 v/v for moisture (Table 2). These climatic thresholds define the

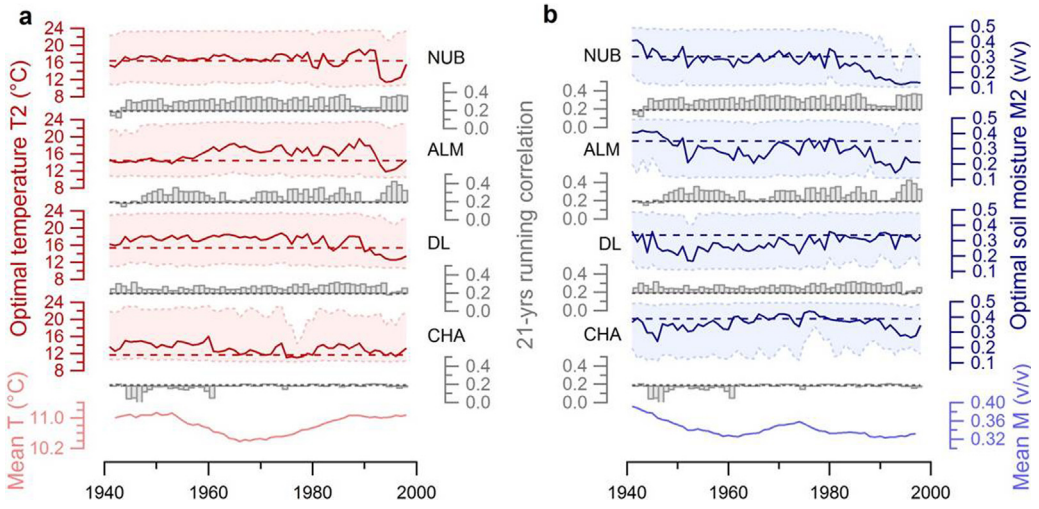

Fig. 4. Estimated optimal temperature (T_2; a) and moisture (M_2; b) for growth parameters over a 21-year sliding window as an indication of the temporal stability of the growth response functions at each site. Horizontal dashed lines indicate the median of the T_2 and M_2 parameters calibrated over the entire period 1931–2008. The red (a) and blue (b) shading denote the 90% credible intervals for the median. Growing season temperature and moisture averaged over each 21-year sliding window are shown in the bottom panels to facilitate the interpretation of changes in parameters over time. The grey bars denote the correlations (1931–2008) between the actual tree-ring width chronologies and those simulated with the parameters calibrated over the corresponding 21-year sliding window. The bars above the line are significant at 95% confidence level. (For interpretation of the references to colour in this figure legend, the reader is referred to the web version of this article).

Table 3
Intercomparison between actual and simulated tree-ring chronologies. Correlation coefficients are given for the entire period of calibration 1931–2008, the two half of the entire period 1931–1969 and 1970–2008 and for the periods before and after 1976. The one year lagged correlations between simulated and observed tree-ring chronologies over the periods 1970–2008 and 1976–2008 are significant for the most xeric site CHA (r_{lag-1}). The asterisk (*) denotes significance at the 95% confidence level.

	Calib. 1931–1969			Calib. 1931–2008			
Valid.	1931–2008	1931–1969	1970–2008	1931–1969	1970–2008	1931–1975	1976–2008
NUB	0.28*	0.38*	0.17	0.39*	0.34*	0.47*	0.07
ALM	0.27*	0.39*	0.14	0.50*	0.25	0.53*	0.08
DL	0.31*	0.41*	0.18	0.46*	0.16	0.52*	−0.13
CHA	0.16	0.37*	−0.02 r_{lag-1} = 0.39*	0.40*	0.04 r_{lag-1} = 0.43*	0.34*	0.05 r_{lag-1} = 0.44*

growing season in the model and determine the seasonal patterns of climate limitation of tree growth. Nevertheless, it is necessary to consider that these estimates do not account for the difference in elevation between the meteorological station (840 m asl) and the sites (1274–1612 m asl) and thus the temperature thresholds for growth might be overestimated. Likewise, the amount of precipitation falling at the mesic-to-humid sites might be underestimated since the meteorological station is situated at the dry edge of the precipitation gradient and is spatially, and presumably climatically, closer to the driest site.

3.2.2. Simulated tree-ring chronologies and patterns of climate limitation

The simulated tree-ring chronologies are all significantly correlated with the actual tree-ring chronologies over the 77-year study period (r = 0.21 to 0.38; p < 0.05) but the explained variance over this period is less than 15% (Fig. 5a). The overall skill of the model is higher at the two most temperature-limited sites in the wetter part of the gradient (NUB and ALM; r > 0.37) and decreases towards the drier eastern locations (DL and CHA; r < 0.33). Despite using the whole study period for calibration, the model is still unable to correctly simulate tree growth variability after the 1970s at the three wettest sites and after around 1963 at the driest site (Fig. A.3). Correlations between the simulated and actual tree-ring chronologies lose significance at all sites in the 1976–2008 period (Table 3). As discussed in the previous section, this issue is related to the shifts in climate response of tree growth observed at the sites, which the model is not able to represent because of its structure.

The simulated patterns of climate limitation vary consistently along the precipitation gradient, with a pattern of increasing moisture limitation of growth rates towards the east (Fig. 5b). Growth rates tend to be limited by low temperatures (gT < gM) at the beginning and end of the growing season and by soil moisture availability (gM < gT) during the peak of the growing season in the austral summer. At the wettest treeline site (NUB), low temperatures limit growth rates during the entire growing season and summer soil moisture availability becomes limiting only in some years (Fig. 5a–b). Temperature limitation during the peak of the growing season decreases towards the east whilst moisture limitation increases resulting in a mixed pattern of climatic limitation for the mesic and drier sites (Fig. 5b). During drought years, the model tends to overestimate moisture limitation, which results in much narrower simulated rings compared with the actual ring width anomalies (see crosses in Fig. 5a–b).

In order to determine whether the patterns of climatic limitation of simulated tree-ring growth have changed between the wet-warm climate regime prior to 1952 and the subsequent dry cooling period between 1952 and 1975, the mean growth rates due to soil moisture and temperature were compared for the two periods (Fig. 5c). Temperature limitation during the peak of the growing season increased slightly during the cooling period across all sites but the change is not statistically significant (p > 0.1). Likewise, moisture limitation across the sites also increased between 1931 and 1951 and 1952–1975. The change is greater than that of temperature limitation but reaches statistical significance (p < 0.1) only during March and April at two sites (ALM and CHA). Because the simulated growth response is controlled by the point-wise min-

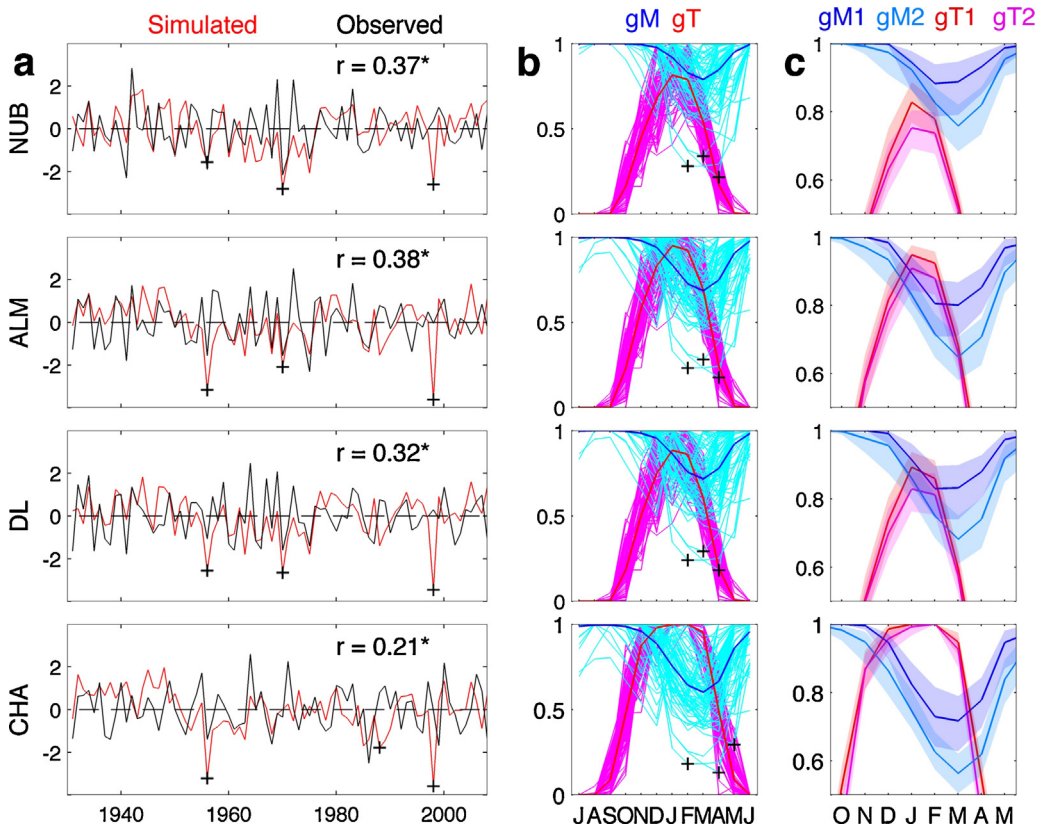

Fig. 5. Intercomparison of actual and simulated tree-ring chronologies together with the associated seasonal patterns of climate limitation simulated by the VS-Lite forward model at each site (NUB, ALM, DL and CHA). (a) Comparison between actual (black) and simulated (red) tree-ring chronologies. Correlation coefficients are given for the period 1931–2008. The asterisk denotes significance at the 95% confidence level. (b) Annual and long-term mean monthly growth rates due to soil moisture (gM, blue) and temperature (gT, purple) for the period 1931–2008. The black crosses in (a) and (b) denote the three years with the strongest simulated moisture limitation for each site. (c) Modelled mean growth rates due to soil moisture and temperature for the wet and warm period 1931–1951 (gM_1 and gT_1) and the cooling period 1952–1976 (gM_2 and gT_2). Shaded regions are 95% bootstrapped confidence intervals about the means, and demonstrate that average growth rates as a function of soil moisture are indistinguishable between the two periods except during the late summer–spring at the three easternmost sites of the gradient (ALM, DL and CHA).

imum of either temperature or moisture, the increasing moisture limitation on tree-growth is effectively felt at the driest site (CHA) rather than at the two sites mentioned above. These results show that despite its limitations, the model can provide useful mechanistic understanding of the complex climate-growth relationships observed at these high-elevation forests.

4. Discussion

4.1. Patterns of tree-ring growth along the moisture gradient

The comparison of the updated tree-ring chronologies with climate variations along the west-to-east precipitation gradient suggests a significant climate control on inter-annual tree-ring growth during the current growing season. However, we found important differences in the responsiveness of tree-ring growth to climate between west and east sides of the precipitation gradient. They are probably due to the effects of water availability on physiology and surface radiation budget.

At mesic-to-humid treelines, above-average *N. pumilio* growth is associated with above-average temperature and below-average precipitation in late spring-early summer (November–January; Fig. 3). The link between temperature-precipitation and growth may arise from the effect of cloudiness. Indeed, cloud cover, limits daytime heating and is often associated to rainfall in Patagonia (Fig. 4; González, 2013), which conditions reduce the incoming solar radiation, decreasing the photosynthetic activity of the trees and thus their carbohydrates production (Rozas et al., 2015). The climatic response of the three mesic populations, as well as the leading EOF of all the chronologies, could thus be primarily influenced by dominant windward fronts from the Pacific Ocean during the growing season. This could be actually the prevailing climatic response throughout the whole gradient. Temperature and precipitation may also affect growth through snow cover. According to Villalba et al. (1997), the snow persistence in spring near the Cerro Tronador, at the western edge of the gradient, indeed depends primarily on November precipitation and temperature. The combination of low precipitation and high temperature during this spring month likely promotes faster snowmelt, which in turn quickens cambial activity and stimulates tree growth.

The VS-Lite model shows a mixed control of growth by temperature and moisture at the intermediate sites (ALM, DL) and an exclusive control by temperature at the humid one. These results do not match strictly the observations. However, if the hypotheses we have put forward are correct, the model, which does not account for cloudiness and snow dynamics cannot fully simulate the climate—growth relations (see 4.3).

In contrast to the three mesic populations, xeric high-elevation treeline forests appear limited by high temperature and low water availability in December and July. Water falling in December alleviates drought stress, which is beneficial to trees. These results are in agreement with Lara et al. (2001; 2005), who showed similar relationships between *N. pumilio* growth and summer conditions at xeric sites in Chile (at 36–39°S). At high-elevations, the precipitation falling mainly as snow in July, a thick snowpack could not only provide snowmelt water but also protect soil from frost, making

melt water infiltration into the soil possible. Therefore, the positive correlation between ring-width and precipitation in July is likely induced by the positive effect of the snow pack accumulation and the consequent soil water recharge (Magnin et al., 2014; Villalba et al., 1997). Consistently, the VS-lite model simulates a dominant control of tree-growth by moisture availability.

4.2. Changes in climate limitation of year-to-year tree-ring growth

According to our data, local climate variations, driven by changes in climate regime, yielded temporal changes of the year-to-year growth-limiting factors. Notably, the positive relation between November–December temperature and growth at the mesic-to-humid sites is enhanced during the dry and cool 1952–1975 period, which may reveal an increase of the snowpack influence on growth. During this time period, at the two wettest sites, the positive relation with soil moisture in spring (September–November) also indicates that water availability, likely released by spring snowmelt, promoted tree-ring growth. At the driest site, warm December temperatures apparently exacerbating moisture limitation had a negative impact on growth. According to the model, the moisture limitation has increased at all sites between the wet-warm climate regime prior to 1952 and the subsequent dry-cool period between 1952 and 1975, but the increase of sensitivity to moisture has been significant only at the driest site. So, at all sites, the growth response functions have undergone some modifications. Nevertheless, from 1931 to ca. 1975, measured and modelled growths are coherent. It means that the effects of environmental parameters like snowpack and cloudiness, not explicitly accounted for by the model, do not introduce bias detrimental to the reconstruction of growth variations through time.

The correlation between growth and December precipitation has been positive at the driest site all over the 1931–2008 period but a positive response of growth to the current and previous year moisture has emerged since the mid-1970s. At the mesic-to-humid sites, the relation between growth and current year soil moisture does not show a clear trend although the correlations with precipitation have turned to positive at ca. 1976. These findings suggest that the impact of humidity (rain, moisture) on growth has not only increased at the dry edge of the precipitation gradient, but has been enhanced along the whole transect. These results are consistent with Suarez et al. (2015) who have observed an increase of the similarity of *Nothofagus dombeyi* growth patterns along the gradient during the last decades.

Whatever the calibration period chosen, the VS-Lite model cannot simulate post-1970s growth variations consistent with the actual tree-ring growth chronologies. As the model proved efficient over the rest of the time period, such a discrepancy suggests that some environmental parameters, which are not taken into account in the model, have reached critical thresholds beyond which growth is significantly impacted. We have proposed above that cloudiness and snowpack can be responsible for changes in tree-ring growth through their effects on radiation, temperature and moisture availability. To our knowledge the temporal changes in cloudiness is not well documented in the region. Data retrieved from the NASA/GEWEX Surface Radiation Budget show that over 1984–2007, the cloud fraction has slightly decreased in summer (−4%) with a concomitant increase of the photosynthetically active radiations (+3.5%; Fig. A.4). These trends are consistent with an increasing effect of cloud cover/radiation on growth. However, they are small and we wonder if such subtle changes can be responsible for the deterioration of the growth-climate relation. Moreover, the records do not go far enough back in time to investigate possible effects in the 1970s. The dependence of growth on snowpack may also be stronger over the recent decades than previously. Indeed, the substantial change of the amount and duration of the snowpack in northern Patagonia in the last decades may have altered the water dynamics in the soil and consequently the tree growth in a sizable way. A well-documented interval of glacier advance culminating in 1976–1977 reported in the north Patagonian Andes, followed by a period of glacier retreat, has taken place in response to changes in climate conditions (Masiokas et al., 2008). Consistently, the snow cover duration has decreased from the late 1970s (at least to the late-1990s, end of the studied period in Villalba et al., 1997). These findings advocates for stronger impact of snowpack on year-to-year tree-ring growth over the recent decades.

Other controlling processes may also explain the apparent lack of the VS-Lite model skill in simulating ring-width over the recent period. For instance, the upward trend of global concentration of atmospheric CO_2 has been increasing at an accelerating rate since the mid-1960s (Robertson et al., 2001). The increase of atmospheric CO_2 concentration may promote tree growth by enhancing the photosynthetic activity and/or reducing the stomatal conductance, leading to the increase of the intrinsic water-use efficiency of trees (e.g., Ainsworth and Rogers, 2007; Keenan et al., 2013). A combination of factors, such as those mentioned above, may be responsible for the decoupling between modelled and measured growth after the 1970s.

4.3. Limitation of the model and perspectives

The moisture in the one-layer Leaky Bucket hydrological model is an estimation of the soil content in the upper 1–2 m (Huang et al., 1996) and integrates the land surface water balance over several months. Schulze et al. (1996) have shown that although *N. pumilio* roots reach ground water at 2-3 m depth, its major water supply comes from the upper soil horizons (at ca. 4 cm depth). So, the actual hydrological module may not be representative of the source water of the trees. However, the overall good agreement we obtain between simulated and measured ring-width before the late 1970s is not consistent with a poor adequacy of the hydrological module. A possible explanation, which would deserve additional investigations, could be that the depth of the water reservoir impacts the tree growth in a sizable way only when the water supply is below a certain threshold. If so, using a multiple layer hydrological module may alleviate the post-late 1970s discrepancy between observed and simulated ring-width chronologies.

The difficulty to reproduce tree-ring growth using the VS-Lite model may also be inherent to its structure and parametrization. For instance, the model lacks upper limits for optimal temperature and moisture. As a result, an optimal growth is simulated even in extremely warm or humid years, which may not reflect the reality. Another structural weakness is the failure to take into account lagged effects while, in the Patagonian context, the previous year conditions have proved to influence growth (this study and e.g., Aravena et al., 2002; Villalba et al., 2003). The full process-based Vaganov–Shashkin model (Vaganov et al., 2006), which simulates daily cambial dynamics and xylem growth, or even more complex eco-physiological models, such as TREERING2000 (Fritts et al., 2000) or MAIDEN (Misson, 2004), are able to link photosynthesis and carbohydrate allocation to stem growth and integrate a higher number of processes and controlling factors. They are certainly more efficient for analyzing tree growth-climate relationships. However, some of them are designed for coniferous trees (Vaganov–Shashkin and TREERING2000), which prevent running them for *N. pumilio*, and all of them operate with daily data, which preclude their use in poorly documented remote regions such as Patagonia. Ongoing monitoring of tree physiology, environmental conditions, and wood cell formation will provide a more detailed

representation of the complex biological and ecological processes operating in the Patagonian sites.

5. Conclusions

We have assessed the year-to-year responses of *N. pumilio* growth to recent changes in climate regimes (1931–2008) along the steep precipitation gradient of northern Patagonia. The combine use of statistical and forward modelling analyses has allowed detecting substantial changes in the sensitivity of tree-ring growth through time, coincident with shifts in climate regimes. Humidity control on growth has increased, and this limitation has been more significant at the xeric than at the mesic sites.

Over the 1931- mid-1970s period, the VS-Lite model has skills to reproduce the tree-ring variations. From the mid-1970s onwards, simulated and measured tree-ring growths are not consistent. We hypothesize that some environmental parameters (cloudiness, snowpack, atmospheric CO_2), whose variations are not explicitly taken into account in the model, have reached critical thresholds impacting tree-growth. Beside, by design, the model itself may not be able to generate realistic tree-ring width over a certain temperature threshold.

Ongoing monitoring of tree-growth and climate will provide the input and control data necessary to run more sophisticated models in order to quantify the impact of various environmental parameters on growth and simulate their effects in projected climatic conditions.

Acknowledgments

This research has being supported by LEFE-PATISO project from CNRS-INSU and by a grant from University of Versailles—St Quentin (France). We thank the IANIGLA team for the assistance for fieldwork, L. Bianchi, M. R. Radins and M. Rodriguez Catón for providing some updated *N. pumilio* chronologies, A. Srur for her helpful attention during the dendrochronological procedures, O. Mestre and B. Dubuisson from Météo-France for assistance with the HOMER software and two anonymous reviewers for their constructive suggestions to improve the manuscript.

Appendix

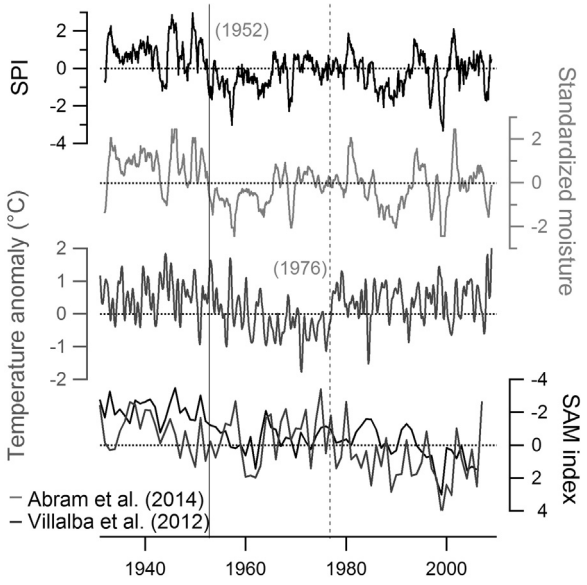

Fig. A.1. Temporal variations in local monthly climate forcing from the Bariloche meteorological station and SAM index. The timing of significant change points (Beaulieu et al., 2012) in the mean of precipitation and temperature series is indicated by the vertical lines (1952 and 1976). From top to bottom: 12-month standardized precipitation index (SPI), 12-month standardized soil moisture derived from the VS-Lite model, monthly temperature anomalies relative to the historical mean (wrt 1961–1990) and the historical (Abram et al., 2014) and tree-ring reconstructed (Villalba et al., 2012) SAM index. Note that the later is plotted with reversed *y*-axis to aid comparison with the local climate series.

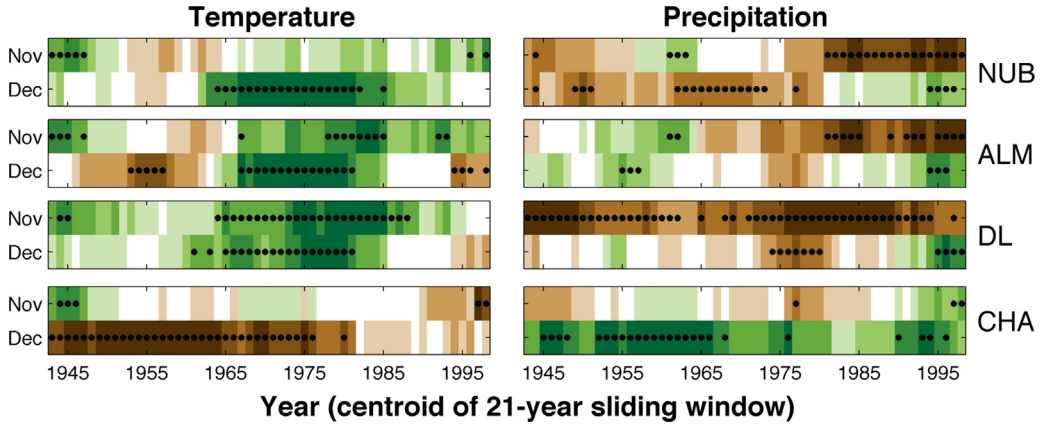

Fig. A.2. Temporal patterns of correlation between *N. pumilio* tree-ring growth and November and December temperature and precipitation from April of the previous growing year (p) to December of the current growing year. Correlations are shown for 21-year running windows. The stippling denotes significant correlations at the 90% confidence level ($p < 0.1$).

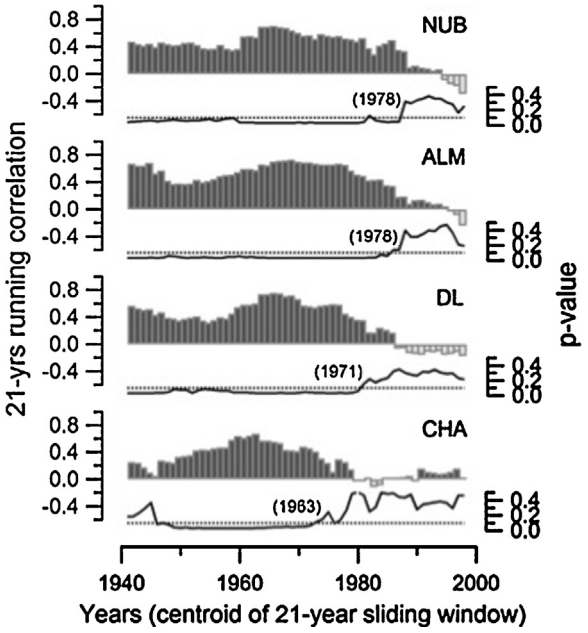

Fig. A.3. Correlations between simulated and actual tree-ring chronologies over a 21-year sliding window. The model was calibrated over the whole period 1931–2008. The dashed lines denote significance at the 90% confidence level ($p < 0.1$). The years in parentheses correspond to the approximate time when the model loses its ability to simulate tree-ring growth based on the significance of the correlations.

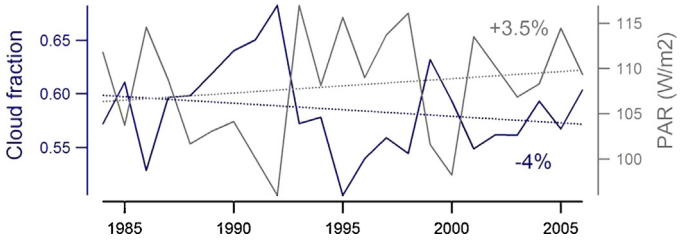

Fig. A.4. Covariations of photosynthetically active radiation (PAR, irradiance in W/m^2) and cloud fraction (in %) in summer months (December–March). Data were retrieved from the NASA/GEWEX Surface Radiation Budget (SRG) Release-3.0 dataset (https://eosweb.larc.nasa.gov/project/srb/srb_rel3.0_sw_monthly_local_nc_table).

References

Abram, N.J., Mulvaney, R., Vimeux, F., Phipps, S.J., Turner, J., England, M.H., 2014. Evolution of the Southern Annular Mode during the past millennium. Nat. Clim. Change 7, 564–569.

Aceituno, P., 1988. On the functioning of the Southern Oscillation in the South American sector. Part I: surface climate. Mon. Weather Rev. 116, 505–524.

Ainsworth, E.A., Rogers, A., 2007. The response of photosynthesis and stomatal conductance to rising [CO_2]: mechanisms and environmental interactions. Plant Cell Environ. 30, 258–270.

Allen, K.J., Cook, E.R., Buckley, B.M., Larsen, S.H., Drew, D.M., Downes, G.M., Francey, R.J., Peterson, M.J., Baker, P.J., 2014. Continuing upward trend in Mt Read Huon pine ring widths—temperature or divergence? Quat. Sci. Rev. 102, 39–53.

Allen, K.J., Cook, E.R., Francey, R.J., Michael, K., 2001. The climatic response of *Phyllocladus aspleniifolius* (Labill.) Hook. f in Tasmania. J. Biogeogr. 28, 305–316.

Álvarez, C., Veblen, T.T., Christie, D.A., González-Reyes, Á., 2015. Relationships between climate variability and radial growth of Nothofagus pumilio near altitudinal treeline in the Andes of northern Patagonia, Chile. For. Ecol. Manage. 342, 112–121.

Anchukaitis, K.J., Evans, M.N., Kaplan, A., Vaganov, E.A., Hughes, M.K., Grissino-Mayer, H.D., Cane, M.A., 2006. Forward modeling of regional scale tree-ring patterns in the southeastern United States and the recent influence of summer drought. Geophys. Res. Lett. 33, L04705.

Aravena, J.C., Lara, A., Wolodarsky-Franke, A., Villalba, R., Cuq, E., 2002. Tree-ring growth patterns and temperature reconstruction from *Nothofagus pumilio* (Fagaceae) forests at the upper tree line of southern Chilean Patagonia. Rev. Chil. Hist. Nat. 75, 361–376.

Archer, C.L., Caldeira, K., 2008. Historical trends in the jet streams. Geophys. Res. Lett. 35, 21–24.

Beaulieu, C., Chen, J., Sarmiento, J.L., 2012. Change-point analysis as a tool to detect abrupt climate variations. Philos. Trans. R. Soc. A. Math. Phys. Eng. Sci 370, 1228–1249.

Boucher, E., Guiot, J., Hatté, C., Daux, V., Danis, P.A., Dussouillez, P., 2014. An inverse modeling approach for tree-ring-based climate reconstructions under changing atmospheric CO_2 concentrations. Biogeosciences 11, 3245–3258.

Breitenmoser, P., Brönnimann, S., Frank, D., 2014. Forward modelling of tree-ring width and comparison with a global network of tree-ring chronologies. Clim. Past 10, 437–449.

Briffa, K.R., 1984. Tree- Climate Relationships and Dendroclimatological Reconstructions in the British Isles. Dissertation. University of East Anglia, Norwich, UK.

Chavardès, R.D., Daniels, L.D., Waeber, P.O., Innes, J.L., Nitschke, C.R., 2013. Unstable climate-growth relations for white spruce in southwest Yukon, Canada. Clim. Change 116, 593–611.

Christie, D.A., Boninsegna, J.A., Cleaveland, M.K., Lara, A., Le Quesne, C., Morales, M.S., Mudelsee, M., Stahle, D.W., Villalba, R., 2011. Aridity changes in the temperate-Mediterranean transition of the Andes since AD 1346 reconstructed from tree-rings. Clim. Dyn. 36, 1505–1521.

Cook, E.R., Buckley, B.M., D'Arrigo, R.D., Peterson, M.J., 2000. Warm-season temperatures since 1600 BC reconstructed from Tasmanian tree rings and their relationship to large-scale sea surface temperature anomalies. Clim. Dyn. 16, 79–91.

D'Arrigo, R.D., Kaufmann, R.K., Davi, N., Jacoby, G.C., Laskowski, C., Myneni, R.B., Cherubini, P., 2004. Thresholds for warming-induced growth decline at elevational tree line in the Yukon Territory, Canada. Global Biogeochem. Cycles 18, GB3021.

Daniels, L.D., Veblen, T.T., 2004. Spatiotemporal influences of climate on altitudinal treeline in northern Patagonia. Ecology 85, 1284–1296.

Donoso, C., 1981. Tipos forestales de los bosques nativos de Chile. In: Documento de Trabajo N°38. Investigación y Desarrollo Forestal (CONAF, PNUD-FAO), FAO, Chile, pp. 70.

Ebisuzaki, W., 1997. A method to estimate the statistical significance of a correlation when the data are serially correlated. J. Clim. 10, 2147–2153.

Evans, M.N., Reichert, B.K., Kaplan, A., Anchukaitis, K.J., Vaganov, E.A., Hughes, M.K., Cane, M.A., 2006. A forward modeling approach to paleoclimatic interpretation of tree-ring data. J. Geophys. Res. 111, G03008.

Evans, M.N., Tolwinski-Ward, S.E., Thompson, D.M., Anchukaitis, K.J., 2013. Applications of proxy system modeling in high resolution paleoclimatology. Quat. Sci. Rev. 76, 16–28.

Evans, M.N., Smerdon, J.E., Kaplan, A., Tolwinski-Ward, S.E., González-Rouco, J.F., 2014. Climate field reconstruction uncertainty arising from multivariate and nonlinear properties of predictors. Geophys. Res. Lett. 41, 9127–9134.

Fritts, H.C., 1976. Tree Rings and Climate. Academic Press, London, pp. 567.

Fritts, H.C., Shashkin, A.V., Hemming, D.L., Leavitt, S.W., Wright, W.E., Downs, G.M., 2000. User manual for TREERING 2000. http://www.ltrr.arizona.edu/~hal/treering/.

Garreaud, R.D., Vuille, M., Compagnucci, R., Marengo, J., 2009. Present-day South American climate. Palaeogeogr. Palaeoclimatol. Palaeoecol. 281, 180–195.

Gillett, N.P., Kell, T.D., Jones, P.D., 2006. Regional climate impacts of the Southern Annular Mode. Geophys. Res. Lett. 33, L23704.

González, M.H., 2013. Some indicators of interannual rainfall variability in Patagonia (Argentina). In: Tarhule, A. (Ed.), Climate Variability—Regional and Thematic Patterns. InTech, pp. 133–161.

Holmes, R.L., 1983. Computer-assisted quality control in tree-ring dating and measurement. Tree-Ring Bull. 43, 69–78.

Huang, J., Van Den Dool, H.M., Georgakakos, K.P., 1996. Analysis of model-calculated soil moisture over the United States (1931–1993) and applications to long-range temperature forecasts. J. Clim. 9, 1350–1362.

Jacoby, G.C., D'Arrigo, R.D., 1995. Tree ring width and density evidence of climatic and potential forest change in Alaska. Global Biogeochem. Cycles 9, 227–234.

Jobbagy, E.G., Paruelo, J.M., Leon, R.J.C., 1995. Estimating the precipitation regime from the distance to the Andes in northwest Patagonia. Ecol. Austral 5, 47–53.

Keenan, T.F., Hollinger, D.Y., Bohrer, G., Dragoni, D., Munger, J.W., Schmid, H.P., Richardson, A.D., 2013. Increase in forest water-use efficiency as atmospheric carbon dioxide concentrations rise. Nature 499, 324–327.

Lara, A., Carlos, A.J., Villalba, R., Wolodarsky-Franke, A., Brian, L., Rob, W., 2001. Dendroclimatology of high-elevation *Nothofagus pumilio* forests at their northern distribution limit in the central Andes of Chile. Can. J. For. Res. 31, 925–936.

López Bernal, P.M., Defossé, G.E., Quinteros, C.P., Bava, J.O., 2012. Sustainable management of Lenga (*Nothofagus pumilio*) forests through group selection system. In: Diez, J.J. (Ed.), Sustainable Forest Management—Current Research. InTech, 45-66.

Magnin, A., Puntieri, J., Villalba, R., 2014. Interannual variations in primary and secondary growth of *Nothofagus pumilio* and their relationships with climate. Trees 28, 1463–1471.

Masiokas, M.H., Villalba, R., Luckman, B.H., Lascano, M.E., Delgado, S., Stepanek, P., 2008. 20th-century glacier recession and regional hydroclimatic changes in northwestern Patagonia. Glob. Planet. Change 60, 85–100.

Meko, D.M., Touchan, R., Anchukaitis, K.J., 2011. Seascorr: a MATLAB program for identifying the seasonal climate signal in an annual tree-ring time series. Comput. Geosci. 37, 1234–1241.

Melvin, T.M., Briffa, K.R., 2008. A signal-free approach to dendroclimatic standardisation. Dendrochronologia 26, 71–86.
Melvin, T.M., Briffa, K.R., 2014a. CRUST: software for the implementation of Regional Chronology Standardisation: part 1. Signal-Free RCS. Dendrochronologia 32, 7–20.
Melvin, T.M., Briffa, K.R., 2014b. CRUST: software for the implementation of Regional Chronology Standardisation: part 2, Further RCS options and recommendations. Dendrochronologia 32, 343–356.
Mestre, O., Domonkos, P., Picard, F., Auer, I., Robin, S., Lebarbier, E., Böhm, R., Aguilar, E., Guijarro, J., Vertachnik, G., Klancar, M., Dubuisson, B., Stepanek, P., 2013. HOMER: a homogenization software—methods and applications. Q. J. Hung. Meteorol. Serv. 117, 47–67.
Misson, L., 2004. MAIDEN: a model for analyzing ecosystem processes in dendroecology. Can. J. For. Res. 34, 874–887.
Mundo, I.A., Roig, F.A., Villalba, R., Kitzberger, T., Barrera, M.D., 2012. *Araucaria araucana* tree-ring chronologies in Argentina: spatial growth variations and climate influences. Trees Struct. Funct. 26, 443–458.
Muñoz, Á., Barichivich, J., Christie, D.Á., Dorigo, W., Sauchyn, D., González-Reyes, Á., Villalba, R., Lara, Á., Riquelme, N., González, M.E., 2014. Patterns and drivers of *Araucaria araucana* forest growth along a biophysical gradient in the northern Patagonian Andes: linking tree rings with satellite observations of soil moisture. Austral Ecol. 39, 158–169.
Ohse, B., Jansen, F., Wilmking, M., 2012. Do limiting factors at Alaskan treelines shift with climatic regimes? Environ. Res. Lett. 7, 015505.
Raffaele, E., Puntieri, J., Martinez, P., Marino, J., Brion, C., Barthélémy, D., 1998. Comparative morphology of annual shoots in seedlings of five *Nothofagus* species from Argentinian Patagonia. Comptes Rendus l'Acad. des Sci. - Ser. III - Sci. la Vie 321, 305–311.
Robertson, A., Overpeck, J., Rind, D., Mosley-Thompson, E., Zielinski, G., Lean, J., Koch, D., Penner, J., Tegen, I., Healy, R., 2001. Hypothesized climate forcing time series for the last 500 years. J. Geophys. Res. 106, 14783–14803.
Rozas, V., Camarero, J.J., Sangüesa-Barreda, G., Souto, M., García-González, I., 2015. Summer drought and ENSO-related cloudiness distinctly drive Fagus sylvatica growth near the species rear-edge in northern Spain. Agric. For. Meteorol. 201, 153–164.
Rusch, V.E., 1993. Altitudinal variation in the phenology of *Nothofagus pumilio* in Argentina. Rev. Chil. Hist. Nat. 66, 131–141.
Schlatter, J., 1994. Requerimientos de sitio para la lenga, *Nothofagus pumilio* (Poepp. et Endl.) Krasser. Bosque 15, 3–10.
Schulman, E., 1956. Dendroclimatic Changes in Semiarid America. University of Arizona Press, Tucson, pp. 142.
Schulze, E.-D., Mooney, H.A., Sala, O.E., Jobbagy, E., Buchmann, N., Bauer, G., Canadell, J., Jackson, R.B., Loreti, J., Oesterheld, M., Ehleringer, J.R., 1996. Rooting depth, water availability, and vegetation cover along an aridity gradient in Patagonia. Oecologia 108, 503–511.
Stokes, M.A., Smiley, T.L., 1968. An Introduction to Tree-ring Dating. University of Chicago Press, Chicago, pp. 73.
Suarez, M.L., Villalba, R., Mundo, I.A., Schroeder, N., 2015. Sensitivity of *Nothofagus dombeyi* tree growth to climate changes along a precipitation gradient in northern Patagonia, Argentina. Trees 29, 1053–1067.
Tolwinski-Ward, S.E., Evans, M.N., Hughes, M.K., Anchukaitis, K.J., 2011. An efficient forward model of the climate controls on interannual variation in tree-ring width. Clim. Dyn. 36, 2419–2439.
Tolwinski-Ward, S.E., Anchukaitis, K.J., Evans, M.N., 2013. Bayesian parameter estimation and interpretation for an intermediate model of tree-ring width. Clim. Past 9, 1481–1493.
Vaganov, E.A., Hughes, M.K., Shashkin, A.V., 2006. Growth Dynamics of Conifer Tree Rings: Images of Past and Future Environments. Springer, Berlin, Heidelberg, pp. 354.
Vaganov, E.A., Anchukaitis, K.J., Evans, M.N., 2011. How well understood are the processes that create dendroclimatic records? A mechanistic model of the climatic control on conifer tree-ring growth dynamics. In: Hughes, M.K., Swetnam, T.W., Diaz, H.F. (Eds.), Dendroclimatology. Progress and Prospects. Springer, pp. 37–75.
Veblen, T.T., 1979. Structure and dynamics of *Nothofagus* forests near timberline in South-Central Chile. Ecology 60, 937–945.
Venema, V.K.C., Mestre, O., Aguilar, E., Auer, I., Guijarro, J.A., Domonkos, P., Vertacnik, G., Szentimrey, T., Stepanek, P., Zahradnicek, P., Viarre, J., Muller-Westermeier, G., Lakatos, M., Williams, C.N., Menne, M.J., Lindau, R., Rasol, D., Rustemeier, E., Kolokythas, K., Marinova, T., Andresen, L., Acquaotta, F., Fratiannil, S., Cheval, S., Klancar, M., Brunetti, M., Gruber, C., Prohom Duran, M., Likso, T., Esteban, P., Brandsma, T., Willett, K., 2013. Benchmarking homogenization algorithms for monthly data. AIP Conference Proceedings, 1060–1065.
Villalba, R., Boninsegna, J.A., Veblen, T.T., Schmelter, A., Rubulis, S., 1997. Recent trends in tree-ring records from high elevation sites in the andes of northern Patagonia. Clim. Change 36, 425–454.
Villalba, R., Lara, A., Boninsegna, J.A., Masiokas, M., Delgado, S., Aravena, J.C., Roig, F.A., Schmelter, A., Wolodarsky, A., Ripalta, A., 2003. Large-scale temperature changes accross the Southern Andes: 20th-century variations in the context of the past 400 years. Clim. Change 59, 177–232.
Villalba, R., Lara, A., Masiokas, M.H., Urrutia, R., Luckman, B.H., Marshall, G.J., Mundo, I.A., Christie, D.A., Cook, E.R., Neukom, R., Allen, K.J., Fenwick, P., Boninsegna, J.A., Srur, A.M., Morales, M.S., Araneo, D., Palmer, J.G., Cuq, E., Aravena, J.C., Holz, A., LeQuesne, C., 2012. Unusual Southern Hemisphere tree growth patterns induced by changes in the Southern Annular Mode. Nat. Geosci. 5, 793–798.
Wigley, T.M.L., Briffa, K.R., Jones, P.D., 1984. On the average value of correlated time series, with applications in dendroclimatology and hydrometeorology. J. Clim. Appl. Meteorol. 23, 201–213.
Zhao, M., Heinsch, F.A., Nemani, R.R., Running, S.W., 2005. Improvements of the MODIS terrestrial gross and net primary production global data set. Remote Sens. Environ. 95, 164–176.